Alongshore Coherence at Low Frequencies in Currents Observed Over the Continental Shelf off Oregon and Washington

ADRIANA HUYER

Ocean and Aquatic Affairs, Environment Canada, Ottawa, Canada

BARBARA M. HICKEY AND J. DUNGAN SMITH

Department of Oceanography, University of Washington, Seattle, Washington 98195

ROBERT L. SMITH AND R. DALE PILLSBURY

School of Oceanography, Oregon State University, Corvallis, Oregon 97331

Current observations over the continental shelf at locations off central Oregon and southern Washington had the period from July 18 to September 18, 1972, in common. Low-frequency fluctuations (less than one cycle per day) in the currents are compared by means of visual display, linear regression, and spectral analysis. The currents are found to be highly coherent over an alongshore separation of 200 km. Coherent signals occur at 0.16, 0.3, and 0.44 cpd. The signal at 0.16 cpd occurs with high mutual coherence in wind, current, and sea level and may be a forced shelf wave driven by the wind. The signal at 0.3 cpd has high coherence between current and sea level and may be a free shelf wave generated by the wind. Correlation between observations is higher for separations in the alongshore direction than in the offshore direction in spite of greater separations.

INTRODUCTION

There is considerable energy at periods of several days in current observations over the continental shelf off Oregon [*Cutchin and Smith,* 1973; *Smith,* 1974]. During the summer of 1972, direct current measurements over the continental shelf were made off southern Washington and central Oregon. The arrays were separated by about 200 km, and the observations are suitable for determining the coherence of low-frequency current fluctuations.

The coherence between current records separated in the alongshore distance is emphasized in this paper. The coherence between current meters at the same location but at different depths and between current meters separated in the offshore direction is also briefly examined. Although we interpret the results in terms of wind and sea level observations, the main purpose of the paper is to demonstrate that current observations separated by 200 km in the alongshore direction exhibit significant coherence at periods of several days.

OBSERVATIONS

Two current meter arrays were moored off southern Washington, one near the shelf edge in about 160 m of water (UWOFF) at 46°50'N, 124°50'W and one nearer shore in 73 m of water (UWIN) at 46°25'N, 124°20'W (Figure 1). Moorings were deployed July 17, 1972, serviced August 17, 1972, and recovered September 25, 1972. Both arrays included a current meter at about 20 m and a deep current meter (at 66 m at UWIN and 110 m at UWOFF) that appeared to be above the bottom boundary layer.

The observations off central Oregon were made as part of the 1972 Coastal Upwelling Experiment (CUE-1) [*Pillsbury et al.,* 1974*a*]. Two of the CUE arrays, NH-10 at 44°39'N, 124°17'W and NH-20 at 44°39'N, 124°32'W (Figure 1), were deployed in water depths (80 and 142 m) similar to those at the southern Washington arrays. The array at NH-10 was first moored on July 6, 1972, serviced on August 3 and 31, and recovered on September 18, 1972; the 20-m current meter did not function on the last installation. The array at NH-20 was deployed on July 3, 1972, serviced on August 3, and recovered on August 30, 1972. Both arrays included a current meter at 20 m and one near the bottom (at 60 and 120 m, respectively).

Both sets of current meter data were obtained with Aanderaa current meters with a sampling interval of 5 or 10 min. The data were initially filtered to provide hourly values. Gaps due to the servicing of the arrays (all shorter than a day) were filled by a time series whose spectral characteristics were determined from the end of the previous record and the beginning of the following one. This procedure resulted in continuous data records for each of the current meters, of which five overlapped for the period from July 18 to September 18, and all eight overlapped from July 18 to August 30.

Hourly wind observations were available from both areas, at Westport, Washington, and Newport, Oregon. Sea level was obtained from tide gages at Depoe Bay, Oregon, by Oregon State University with a precision of ±0.3 cm; at Toke Point, Washington, by the U.S. Army Corps of Engineers with a precision of ±1 cm; and at Tofino, B. C. (49°10'N, 125°55'W), by the Canadian Hydrographic Service with a precision of ±1 cm. Hourly values were obtained from each location. Sea level exhibits an 'inverted barometer effect' due to variations in atmospheric pressure: sea level changes 1 cm for every 1 mbar change in atmospheric pressure. Sea level was adjusted for this effect using atmospheric pressure observations from Newport, Oregon; Hoaquiam, Washington; and Tofino, B.C.

The hourly current, wind, and adjusted sea level data were filtered by means of a symmetrical cosine filter spanning 121 hours to suppress tidal and inertial oscillations. The half-power point of the filter is 40 hours, and about 95% of the energy is passed at 50 hours. The filtering results in truncating the time series by 2½ days at each end.

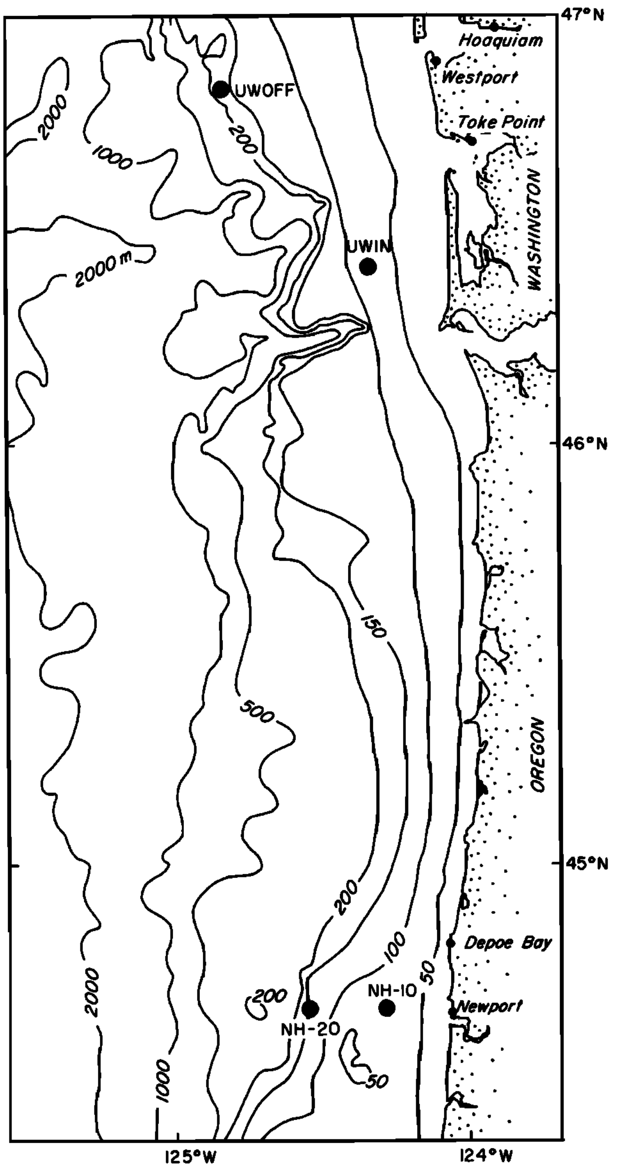

Fig. 1. Locations of current meter arrays and coastal locations of supplementary observations of sea level, wind, and/or atmospheric pressure.

Comparisons Between Current Observations

We compare the current observations by means of visual display, simple statistics, simple linear regression, and spectral analysis. The spectral analysis is restricted to the five current meter records which overlapped for 56 days, while other comparisons are also made for the 37-day period common to all eight current meters.

Comparisons between current meters were made in a 'natural' coordinate system because of significant variations in isobath orientation. Natural coordinates could be taken to be parallel to the local isobath or to be the axes in which the off-diagonal element of the Reynolds stress is zero, i.e., the principal axes. At the deepest current meter in each of the arrays in this study the principal axes were found to be within 5% of the local isobath orientation. We therefore chose to use natural coordinates parallel to the local isobath: 330°T at UWOFF, 347°T at UWIN, and 15°T at both NH-10 and NH-20.

The time series of 6-hourly current vectors are shown in Figure 2 with the wind and adjusted sea level observations. Some of the current records, e.g., 60 m at NH-10, have a mean alongshore component that is nearly zero. Others have northward (e.g., 120 m at NH-20) or southward (20 m at NH-10) mean flows. All records show high variability, a period of about 6 days being most apparent. The fluctuations at all eight current meters appear to be somewhat similar, the greatest similarity occurring between the inshore current meters.

Simple statistics of the currents and their components in both the east-north and the local (natural) reference frames are shown in Table 1 for both the 56-day and the 37-day common period. Almost all statistics are very similar for the two time periods. Standard deviations of both speed and the alongshore component are greater for the nearshore than for the offshore current meters. The standard deviation of the alongshore component is greater than that of the onshore component; in most cases the difference is greater than a factor of 2. At all four locations the mean deep flow was northward relative to the surface flow; this is consistent with previous observations over the Oregon continental shelf in late summer [*Huyer et al.*, 1975].

Simple linear regression. We computed the linear regression and correlation coefficients between the alongshore components of each pair of current meters for both periods. Results are shown (Table 2) for the local isobath coordinate system; they differ only slightly for the northward component. Coefficients were computed from 37 (56) daily values taken at 1200 UT. From analysis of variance [*Panofsky and Brier*, 1963] the probability of uncorrelated populations having a correlation coefficient greater than 0.42 (0.34) is less than 1% for a sample size of 37 (56).

Vertical correlation coefficients are greatest at UWIN and NH-10 and least, but still significant, at UWOFF. The regression coefficient B is near unity at UWIN, NH-10, and NH-20, suggesting that the current fluctuations may be barotropic there, but at UWOFF, fluctuations at the deep current meter have less than half the amplitude of those at the shallow current meter. The mean vertical shear A appears to be greater off central Oregon than off southern Washington. Correlation coefficients are higher between the deep current meters than between shallow current meters. This could be due to the higher variability in lateral density gradients between the shallow current meters (e.g., due to variations in the position of the Columbia River plume) than between the deep current meters. Current fluctuations have smaller amplitudes at the offshore locations ($B < 1$), suggesting that the fluctuations are trapped along the coast. The correlation between the deep current meters is greater for the inshore pair than for the offshore pair, but the correlation between UWIN and NH-20 is also very high.

If the current fluctuation field were isotropic and homogeneous, the correlation coefficient between a pair of current meters would be a function only of the distance between them. Instead, the correlation coefficients with lateral separation are greater for deeper than for shallow current meters. Also the correlation coefficients for alongshore separations are higher than those for offshore separations in spite of much greater alongshore separations.

Alongshore correlation coefficients are lower for UWOFF than for UWIN. This could be due to the greater alongshore separation between UWOFF and the southern current meters, but it is more likely due either to its proximity to the shelf break, to greater offshore separation, or to some local effect at UWOFF. These effects would cause underestimates of the alongshore correlation coefficient. In any case we conclude

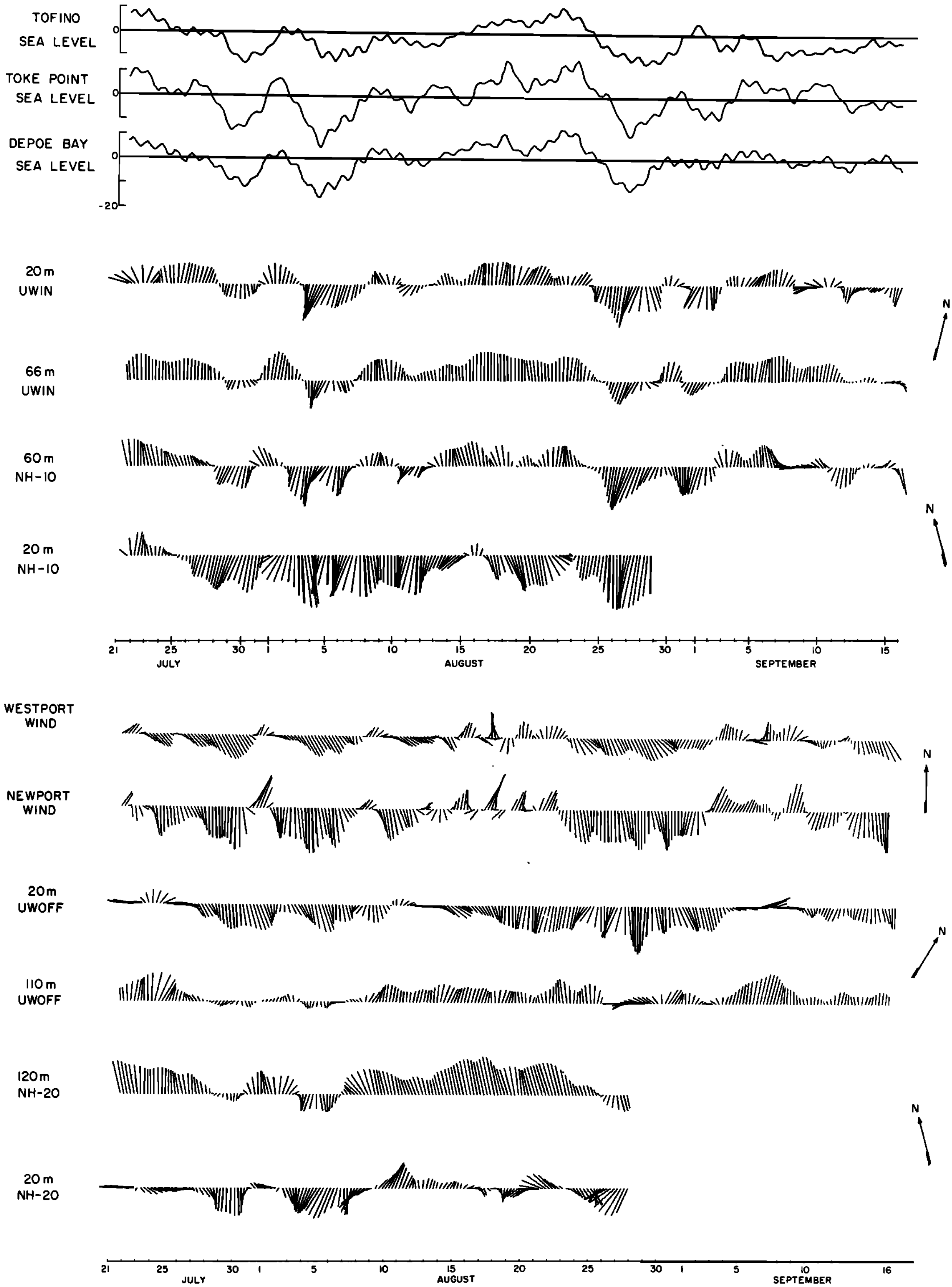

Fig. 2. Time series of 6-hourly vectors of low-passed deep and shallow current, wind and sea level observations, July 21 to September 16. Current vectors are shown in the local isobath coordinate system. Direction of arrow at right indicates true north; its magnitude corresponds to a current speed of 30 cm s^{-1} and a wind speed of 10 m s^{-1}.

TABLE 1. Vector Mean Currents, Principal Axis Angles, and Means and Standard Deviations of Speed and Components in the East-North (u, v) and Local Isobath (u', v') Coordinates, 1800 UT July 21 to 1800 UT August 27, 1972, and (in Parentheses) 1800 UT July 21 to 0000 UT September 16, 1972

	UWOFF		UWIN		NH-10		NH-20	
	20 m	110 m	20 m	66 m	20 m	60 m	20 m	120 m
Vector mean								
Speed, cm s^{-1}	8.9	5.1	1.3	6.7	14.0	2.7	4.0	9.6
	(8.7)	(5.6)	(0.8)	(6.2)		(2.4)		
Direction, °T	141	333	224	343	200	287	213	359
	(136)	(333)	(265)	(348)		(272)		
Principal axis angle, deg	16.5	15.2	0.0	8.0	−17.0	−21.6	−36.1	−6.9
	(33.4)	(20.2)	(0.1)	(9.7)		(−20.5)		
Means								
Speed	11.3	6.8	10.0	10.6	16.5	10.6	9.5	12.5
	(11.1)	(7.1)	(9.5)	(9.7)		(10.2)		
u	5.7	−2.3	−0.9	−1.9	−4.9	−2.6	−2.2	−0.2
	(6.0)	(−2.6)	(−0.8)	(−1.3)		(−2.4)		
v	−6.9	4.6	−1.0	6.4	−13.1	0.8	−3.3	9.6
	(−6.3)	(5.0)	(−0.1)	(6.1)		(0.1)		
u'	1.5	0.3	−0.7	−0.4	−1.4	−2.7	−1.3	−2.3
	(2.0)	(0.3)	(−0.7)	(0.1)		(−2.4)		
v'	−8.5	5.1	1.1	6.6	−14.0	0.1	−3.8	9.4
	(−8.5)	(5.6)	(0.1)	(6.2)		(−0.5)		
Standard deviations								
Speed	4.8	3.9	5.2	4.5	8.5	6.3	6.1	4.7
	(5.1)	(4.0)	(4.8)	(4.7)		(5.6)		
u	4.7	2.4	2.8	2.1	6.0	5.0	8.1	2.7
	(4.4)	(2.4)	(3.3)	(2.4)		(4.6)		
v	7.0	5.4	10.9	9.2	10.8	11.1	8.1	9.0
	(7.4)	(5.4)	(10.1)	(8.5)		(10.4)		
u'	4.6	2.4	3.7	1.9	4.3	2.5	5.9	2.4
	(4.7)	(2.7)	(3.9)	(2.1)		(3.0)		
v'	7.1	5.4	10.6	9.2	11.2	11.7	8.0	9.5
	(7.2)	(5.2)	(9.9)	(8.5)		(10.9)		

that the alongshore correlation length over the continental shelf is at least 300 km for the low-frequency current fluctuations.

Spectral analysis. We use the rotary spectral method described in detail by *Gonella* [1972] and *Mooers* [1973]. In effect, the method decomposes the vector time series into circularly polarized components rotating clockwise and counterclockwise at each frequency. Spectra are then computed for clockwise (negative) and counterclockwise (positive) frequencies. The time series were linearly detrended before the spectra were computed.

The autospectra for the five current records for the period 1800 UT July 21, 1972, to 0000 UT September 16, 1972, are shown in Figure 3. The rotary autospectra show not only at which frequency peaks occur but also whether the current at a particular frequency is more nearly circular or linear and whether it rotates clockwise or counterclockwise. All five spectra show some similarity in that highest energy is observed at lowest frequencies and in that energy tends to decrease as frequency increases. The high-energy low-frequency band is narrowest at UWOFF. Apparent peaks occur at ±0.05 cpd, but since the valley between them is due to the linear detrending of the time series, this should be interpreted simply as a peak at the lowest frequencies. All of the spectra show a peak or shoulder at 0.15 cpd, and three of the spectra (from NH-10 and UWIN) show peaks at 0.3 and 0.45 cpd. Of these three peaks, greatest energy occurs at the lowest frequency and least energy at the highest frequency.

Cross spectra were computed in local isobath coordinates (coherence squared is independent of coordinate rotation, but phase is not). Coherence squared and phase between vertically separated current meters at UWIN and UWOFF are shown in Figure 4. At UWIN the vertical coherence is high over a wide band (−0.55, 0.3 cpd), and it exceeds the coherence at UWOFF at all frequencies. Vertical phase differences are essentially zero wherever the coherence is high and phase estimates are most reliable. This is consistent with the idea that the coherent current fluctuations are approximately barotropic.

Coherence squared and phase spectra for the pairs of deep current meters are shown in Figure 5. Between UWIN and NH-10 there is high coherence over a wide frequency band (−0.5, 0.3 cpd), with a gap in the coherence at −0.35 cpd. Between NH-10 and UWOFF and between UWIN and UWOFF, coherence is lower and restricted to narrower frequency bands. The overall coherence (the integral of the coherence squared spectrum) appears to be about the same for two of the pairs, (UWIN, UWOFF) and (UWIN, NH-10), as we might expect from the similar values of the linear correlation coefficient (0.65 and 0.62).

We investigate further the signals associated with peaks in the autospectra at frequencies of 0.15, 0.3, and 0.45 cpd. Table 3 shows the values of some current ellipse parameters for each of these frequencies: kinetic energy of the rotary components (S_- and S_+) and ellipse stability, orientation [*Gonella,* 1972], and eccentricity [*Mooers,* 1973]. The total kinetic energy ($S_+ + S_-$) at 0.16 cpd is larger than that at 0.3 and 0.44 cpd; the kinetic energy at 0.16 cpd is approximately independent of depth at a given location; at both 0.3 and 0.44 cpd the kinetic energy is greater at the shallower current meters; and the kinetic energy is less at UWOFF than at UWIN or NH-10 for all three signals. The sense of rotation (clockwise or counterclockwise) is given by the sign of the difference in kinetic energy of the two components ($S_+ - S_-$); when the signal is nearly rec-

TABLE 2. Correlation Coefficient (*CC*) and Regression Coefficients (*A* and *B*) Between Pairs of Current Meters

V_1		V_2				
Depth, m	Station	Depth, m	Station	*CC*	*A*	*B*
			Vertical Separation			
20	UWIN	66	UWIN	0.96	5.7	0.83
				(0.95)	(6.1)	(0.82)
20	NH-10	60	NH-10	0.83	12.4	0.88
20	UWOFF	110	UWOFF	0.57	8.9	0.43
				(0.61)	(9.3)	(0.44)
20	NH-20	120	NH-20	0.73	12.5	0.86
			Offshore Separation			
20	UWIN	20	UWOFF	0.40	−9.3	0.27
				(0.48)	(−8.6)	(0.35)
20	NH-10	20	NH-20	0.50	1.5	0.38
60	UWIN	110	UWOFF	0.70	2.4	0.41
				(0.65)	(3.1)	(0.40)
60	NH-10	120	NH-20	0.87	9.3	0.72
			Alongshore Separation			
20	UWIN	20	NH-10	0.68	−15.0	0.69
20	UWOFF	20	NH-20	0.52	1.4	0.60
20	UWIN	20	NH-20	0.56	−4.4	0.43
20	UWOFF	20	NH-10	0.53	−7.1	0.80
66	UWIN	60	NH-10	0.90	−7.5	1.12
				(0.87)	(−7.5)	(1.10)
110	UWOFF	120	NH-20	0.79	1.9	1.41
66	UWIN	120	NH-20	0.95	2.7	0.99
110	UWOFF	60	NH-10	0.68	−7.6	1.46
				(0.62)	(−7.7)	(1.28)

Regression equation is $V_2 = A + BV_1$. Values are given for the period July 21 to August 27, 1972, and (in parentheses) for July 21 to September 15, 1972.

tilinear this difference becomes very small and its sign indeterminate. We observe clockwise rotation ($S_- > S_+$) in all cases except at 0.16 cpd at UWIN, where the signal is strong and approximately linear.

Ellipse stability [*Gonella*, 1972] is low for nearly circular motion or if the orientation of the major axis varies appreciably. Ellipse orientation is shown when stability exceeds the 95% significance level (0.53). Ellipse eccentricity, $2(S_- \, S_+)^{1/2} \, (S_- + S_+)^{-1}$ [*Mooers*, 1973], is equal to one for rectilinear motion and to zero for circular motion.

We interpret the values of these ellipse parameters to describe the properties of the three signals. The signal at 0.16

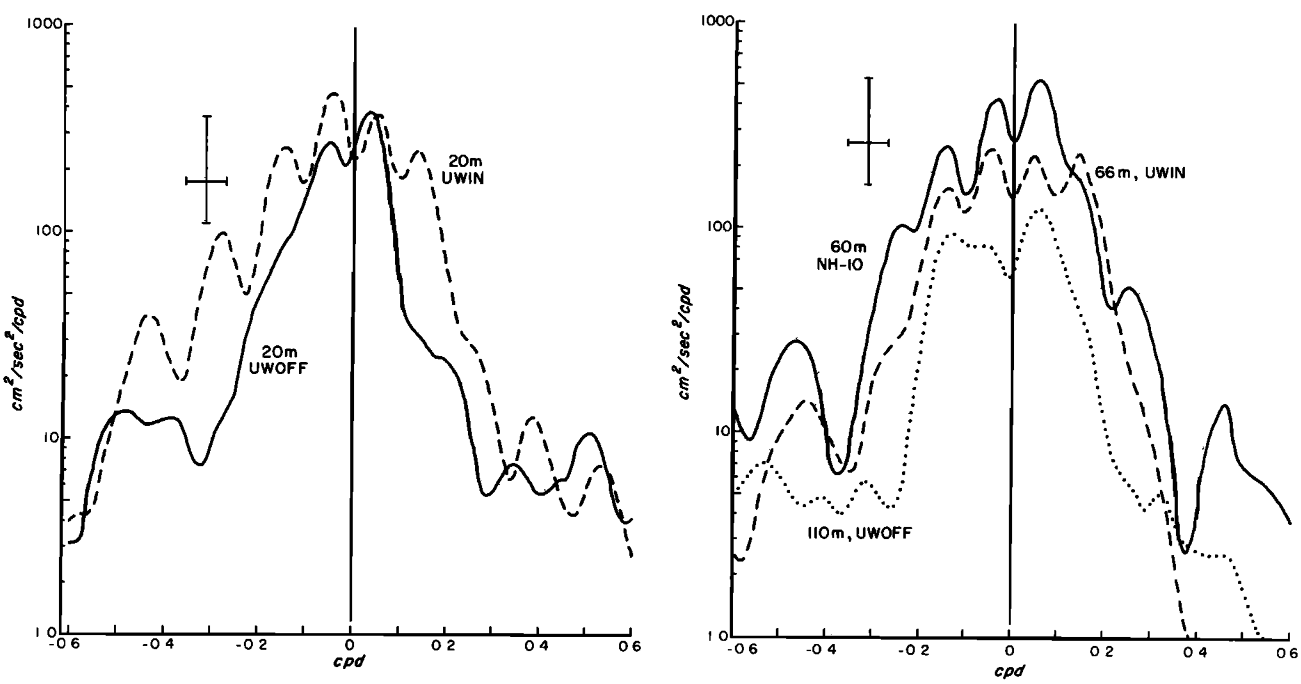

Fig. 3. Autospectra of the current records, July 21 to September 16, 1972, with the 80% confidence interval and the band width.

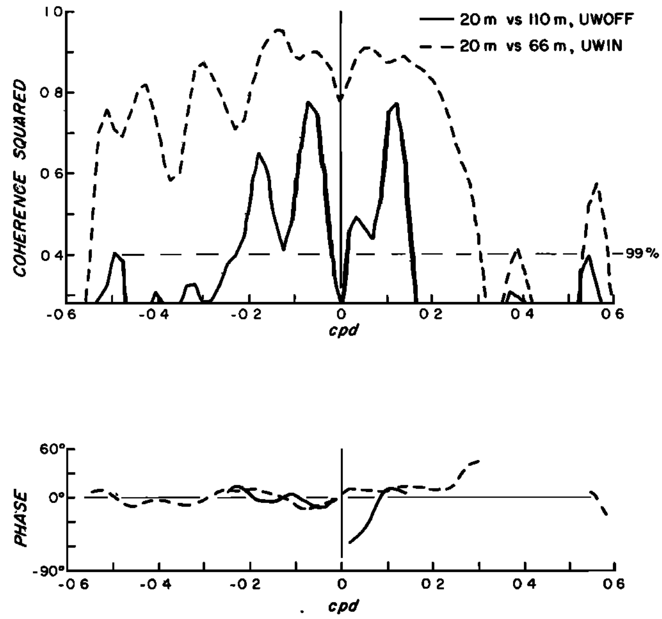

Fig. 4. Coherence squared and phase spectra for vertically separated current meters. Coherence squared values less than the 95% significance level (0.28) are not shown. Phase is shown only when coherence squared exceeds the 99% significance level (0.4). When phase is positive, the second series leads the first.

cpd is the strongest of the three. Its eccentricity appears to decrease as water depth (or distance offshore) increases; i.e., it is more circular further from shore, and it is approximately barotropic. Both the kinetic energy at a given depth and its integral over the water column appear to decrease as water depth (distance offshore) increases; i.e., the signal at 0.16 cpd appears to be trapped along the coast. The signals at 0.3 and 0.44 cpd are much weaker. Both appear to have higher energy at the shallower current meters, and they may be baroclinic. The signal at 0.3 cpd seems to be nearly rectilinear at UWOFF and more elliptical at NH-10 and UWIN. The signal at 0.44 cpd may be circular everywhere.

Each of these signals showed high coherence between several pairs of current meters. Figure 6 shows values of the coherence squared between each pair of current meters, including vertical, offshore, and alongshore separations. Relatively low values are observed for the counterclockwise components at 0.3 and 0.44 cpd (which have low kinetic energy); the maximum value is 0.52 at +0.3 cpd and 0.57 at 0.44 cpd. Alongshore coherence values are high at ±0.16, −0.3, and −0.44 cpd for the inshore current meters, and some offshore coherence is observed for each of these signals.

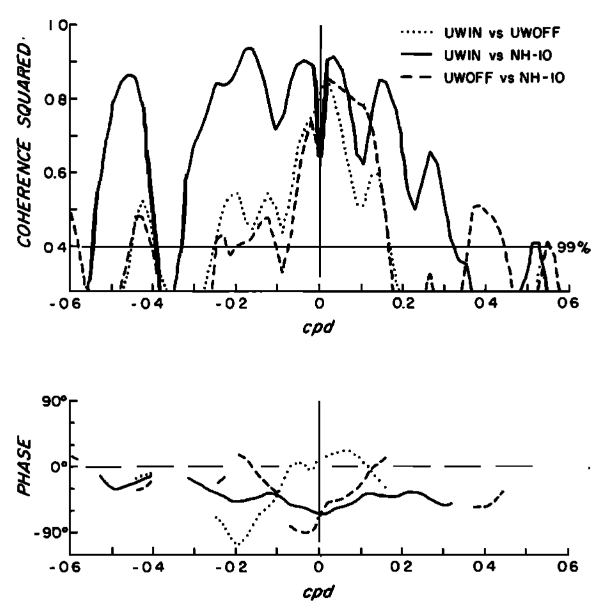

Fig. 5. Coherence squared and phase spectra for the pairs of deep current meters.

COMPARISON WITH WIND AND SEA LEVEL OBSERVATIONS

From the results of earlier studies, e.g., *Huyer and Pattullo* [1972], *Cutchin and Smith* [1973], and *Smith* [1974] we expect the current fluctuations to be related to fluctuations in wind and sea level. Figure 2 shows some similarity between the wind and offshore currents but greater similarity between the wind and the inshore currents. Sea level fluctuations closely resemble the fluctuations in the alongshore component of the current, high sea level being associated with poleward flow. Correlation coefficients between current and sea level and between wind and current (Table 4) are higher for the deep current meters than for shallow current meters. Current fluctuations are more highly correlated with sea level than with wind. A sea level change of 1 cm at Depoe Bay is associated with a change in current velocity of 1.6 cm s^{-1} at NH-10 and 1.5 cm s^{-1} at NH-20; a sea level change of 1 cm at Toke Point is associated with current changes of 1 cm s^{-1} at UWIN and 0.5 cm s^{-1} at UWOFF. At UWIN, current fluctuations have about 4% of the amplitude of wind fluctuations observed at Westport; at NH-10 current changes are 2% of Newport wind changes.

The alongshore correlation and regression coefficients for the wind and sea level observations are shown in Table 5. The high linear correlation coefficients indicate not only that the dominant signals are coherent but also that the phase difference in the dominant signals must be relatively small. Fluctuations in the wind at Westport have less than half the amplitude of those at Newport; this accounts for the difference in the ratio between current and wind amplitudes, since current fluctuations at UWIN and NH-10 have about the same amplitude (Table 2). Alongshore correlation coefficients are about the same for sea level and the deep currents, lower for the wind, and least for the shallow currents for comparable separation between observations.

Rotary autospectra of the low-passed wind observations at Newport and Westport and the coherence squared and phase spectra between them are shown in Figure 7. Since the coast is aligned nearly north-south at both locations, east-north coordinates were used. The wind is more to the left and weaker at Westport than at Newport (Figures 2 and 7, Table 5). The decrease in speed and the change in direction are consistent with the general northward decrease in zonal wind stress in summer [*Bakun*, 1973] associated with the mean position of the North Pacific high pressure system.

Autospectra of the wind (Figure 7) and current (Figure 3) are somewhat similar, but the decrease in kinetic energy with frequency is more gradual for the wind. The wind shows relatively low kinetic energy at 0.3 cpd, while the shallow currents show fairly high energy at this frequency. The alongshore coherence at 0.3 cpd is very low for the wind but significant for the inshore currents (see Figure 6). At other frequencies, including 0.16 and 0.44 cpd, the alongshore coherence of the wind is high.

Autospectra and the coherence squared and phase spectra of sea level observations are shown in Figure 8. The sea level

TABLE 3. Kinetic Energy ($cm^2/s^2/cpd$) of Clockwise (S_-) and Counterclockwise (S_+) Components and Ellipse Stability (s), Orientation (ϕ) in Degrees True, and Eccentricity (e) At Selected Frequencies

Depth,		0.16 cpd					0.3 cpd					0.44 cpd				
m	Station	S_-	S_+	s	ϕ	e	S_-	S_+	s	ϕ	e	S_-	S_+	s	ϕ	e
20	UWOFF	81	28	0.02		0.873	10	6	0.02		0.97	12	7	0.05		0.96
110	UWOFF	82	32	0.78	356	0.898	5	5	0.29		1.00	4	3	0.01		0.99
60	NH-10	232	140	0.93	26	0.968	38	29	0.77	14	0.99	25	12	0.79	357	0.94
66	UWIN	142	190	0.99	359	0.989	17	10	0.47		0.96	14	1	0.35		0.50
20	UWIN	216	189	0.88	4	0.998	77	13	0.30		0.70	35	5	0.06		0.66

autospectra closely resemble those of the deep currents (Figure 3). Coherence squared for sea level is high at 0.16 cpd both between Toke Point and Depoe Bay and between Tofino and Depoe Bay. At 0.33 cpd the coherence is significant, although at 0.3 cpd it is very low between Tofino and Depoe Bay. The bandwidth of the spectral estimates is about 0.08 cpd, and we assume that the coherence peak at 0.33 cpd in sea level is associated with the peak at 0.3 in currents. At 0.44 cpd there is significant coherence between Toke Point and Depoe Bay but not between Tofino and Depoe Bay.

Figure 9 shows the coherence squared spectra between the deep currents and the nearby wind and adjusted sea level observations. Sea level is highly coherent with the inshore current meters over a wide range of frequencies, but coherence

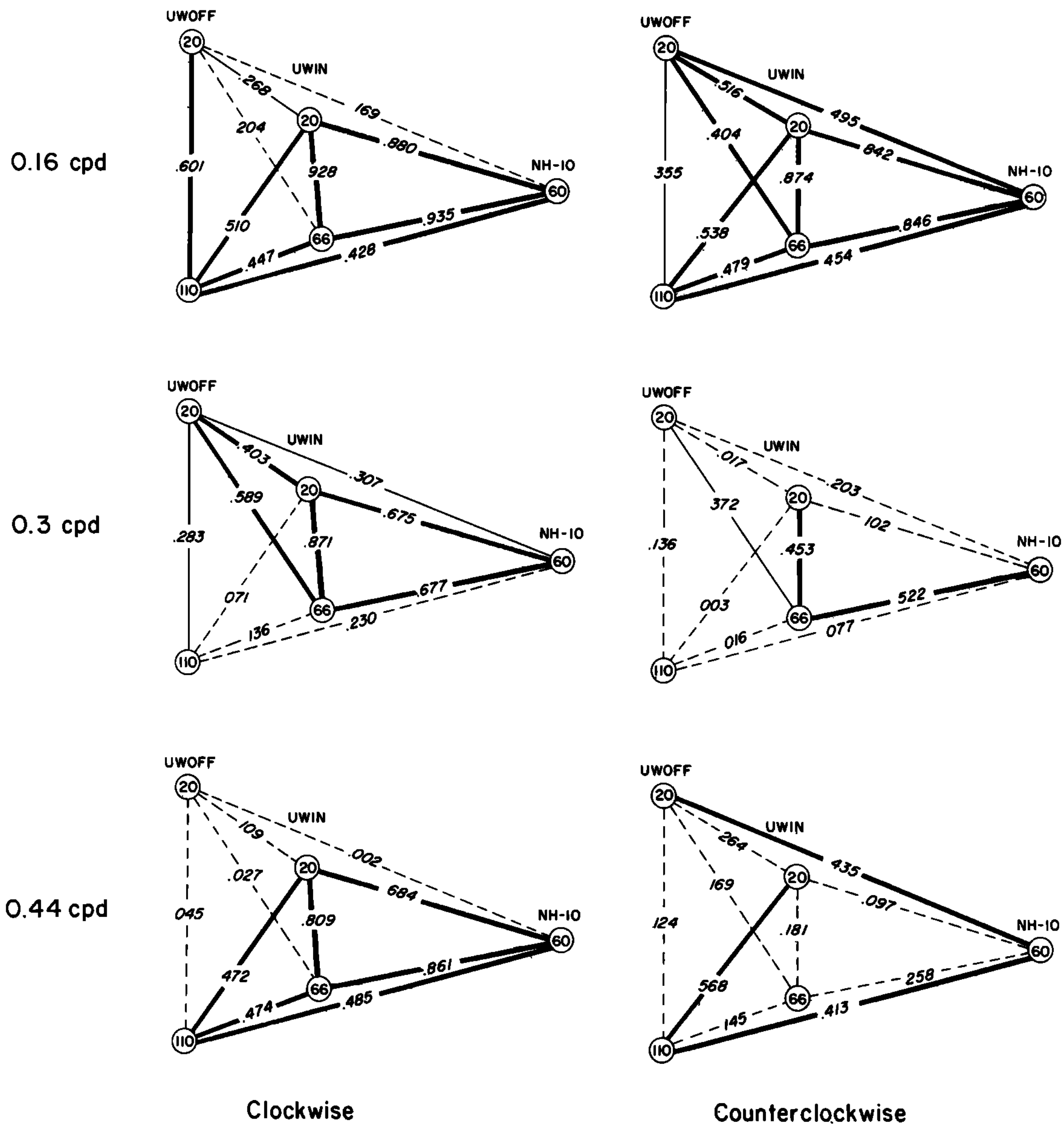

Fig. 6. Values of coherence squared between all pairs of current meters at selected frequencies. A heavy solid line indicates that coherence squared exceeds the 99% significance level, a thin line indicates that is is between the 95% and 99% levels, and a dashed line indicates that the coherence squared between a pair of current meters is not significantly different from zero at the 95% level.

TABLE 4. Correlation Coefficients and Slope of the Regression Lines Between the Alongshore Component of the Current and Adjusted Sea Level and Between Current and the Northward Component of Winds

Location of Observations				Sea Level, Current		Wind, Current	
		Current					
Sea Level	Wind	Depth, m	Station	*CC*	*B*, s^{-1}	*CC*	*B*, cm/m
Toke Point	Westport	20	UWIN	0.81	1.13	0.67	3.6
				(0.79)	(1.12)	(0.62)	(2.95)
		20	UWOFF	0.29	0.28	0.15	0.52
				(0.36)	(0.37)	(0.41)	(1.41)
		66	UWIN	0.89	1.06	0.72	3.33
				(0.87)	(1.06)	(0.67)	(2.77)
		110	UWOFF	0.74	0.51	0.43	1.16
				(0.68)	(0.50)	(0.47)	(1.15)
Depoe Bay	Newport	20	NH-10	0.65	1.16	0.40	1.07
		20	NH-20	0.72	0.95	0.44	0.91
		60	NH-10	0.87	1.64	0.68	1.99
				(0.82)	(1.71)	(0.68)	(1.84)
		120	NH-20	0.94	1.46	0.66	1.60

Values are given for the periods July 21 to August 27, 1972, and (in parentheses) for July 21 to September 15, 1972.

between the offshore deep current and sea level is low at most frequencies. Coherence between the inshore deep currents and the wind is high at low frequencies. The offshore deep current meter shows little coherence with the wind at any frequency. The coherence squared spectra between wind and sea level are quite different for the two locations. At 0.16 cpd there is high coherence between inshore currents and sea level and between inshore currents and wind at both locations; coherence between wind and sea level is high only off central Oregon. At 0.3 cpd, there is high coherence between inshore current and sea level at both locations; coherence between inshore current and wind is high off central Oregon but low off southern Washington. Off Oregon, coherence is high in both rotary components between wind and inshore current and also between current and sea level. For a pure continental shelf wave we expect high coherence only in the clockwise component, as is observed off southern Washington. It seems possible that the signal is generated by the wind off Oregon and that it propagated northward as a wave. At 0.45 cpd, coherence between wind and current is very low, although coherence between sea level and current and between wind and sea level is significant at both locations.

The alongshore coherence is higher for the deep current than for wind and sea level at each of these frequencies (Figures 5, 7, 8). At 0.16 cpd the clockwise components are nearly equally coherent, but in the counterclockwise components the current shows greater alongshore coherence than the wind: this is likely because the current is constrained to be nearly linear by the coast, while the wind is not. At 0.3 cpd there is significant alongshore coherence in both current and

TABLE 5. Correlation Coefficient and Slope of Regression Lines Between Wind Observations and Between Adjusted Sea Level at Different Locations for the Periods July 21 to August 27, 1972, and (in Parentheses) for July 21 to September 15, 1972

	CC	*B*
Wind		
Newport, Westport	0.80	0.40
	(0.81)	(0.42)
Sea level		
Depoe Bay, Toke Point	0.92	1.17
	(0.89)	(1.21)
Depoe Bay, Tofino	0.86	0.74
	(0.75)	(0.68)
Toke Point, Tofino	0.84	0.57
	(0.66)	(0.44)

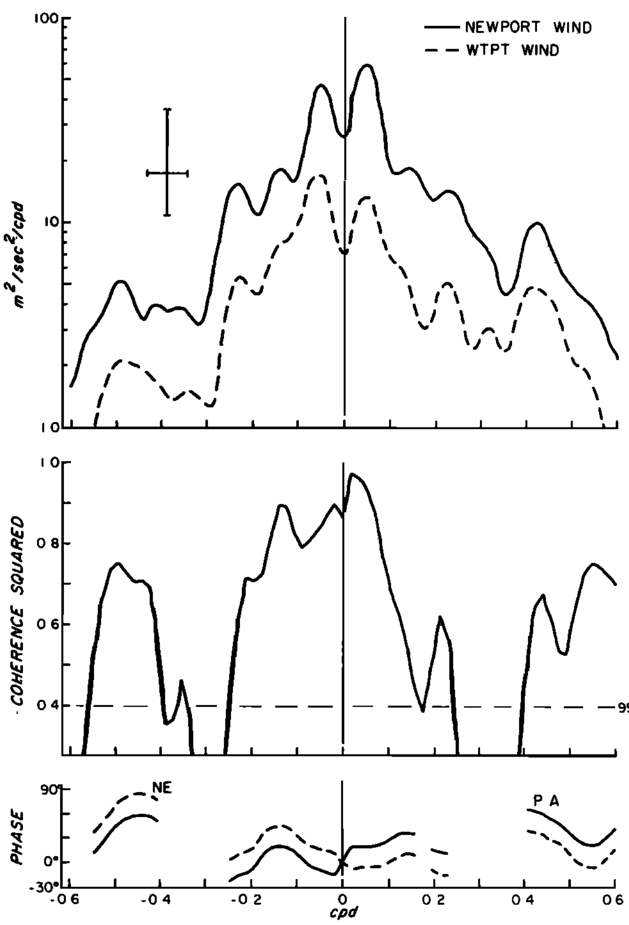

Fig. 7. Autospectra of the wind observations at Newport and Westport and their coherence squared and phase spectra (in principal axes and east-north coordinates). Positive phase indicates that Newport leads Westport.

sea level but not in the wind. This supports the earlier suggestion that this signal may propagate northward like a wave. Earlier we showed that the kinetic energy at this signal was greater at shallow than at deep current meters and hence that the wave is not strictly barotropic. The signal at 0.44 cpd shows high alongshore coherence in both wind and current and lower but still significant alongshore coherence in sea level. This signal is also stronger at the shallow current meters and hence also has a baroclinic component.

Phase spectra of pairs of vector components measured at different locations were used to estimate the time lags and hence wavelength and phase speed and direction. The uncertainty in phase and hence in wavelength and phase speed depends on the number of degrees of freedom (10, in our case) of the spectral estimates and on the value of coherence squared [*Jenkins and Watts,* 1968]. Table 6 shows values of the alongshore coherence squared and phase with its 95% confidence limits for the three signals at 0.16, 0.3, and 0.44 cpd as computed from the wind, adjusted sea level, and deep inshore current observations. The phase difference in the current observations is not highly sensitive to the choice of coordinate systems. At each frequency and for each parameter the observations off central Oregon lead those off southern Washington; i.e., the signals appear to propagate northward.

At 0.16 cpd the 95% confidence limits for phase result in a large range of possible wavelengths: from a minimum of 1680 km (from the sea levels at Tofino and Toke Point) to infinite wavelength (from sea levels at Toke Point and Depoe Bay). There is, however, a wavelength interval that is common for all current, wind, and sea level pairs: from 3390 to 3790 km. The corresponding phase speeds are between 540 and 610 km/day. We tentatively conclude that the signal at 0.16 cpd has the same wavelength and phase speed in wind, current, and sea level. Its wavelength appears to be about 3500 km, and it seems to propagate northward with a phase speed of about 575 km/day.

At 0.3 cpd both current and sea level show significant alongshore coherence between southern Washington and central Oregon, but wind does not. Although coherence is significantly different from zero at the 99% level, the values are not high, and uncertainty in the phase estimates is large. The 95% confidence intervals of phase yield a common wavelength interval from 1360 to 14,400 km with a corresponding phase speed interval from 630 to 4320 km/day. The signal is not sufficiently coherent to enable us to determine its wavelength and speed within reasonable limits from the present data set. Perhaps longer records would yield improved resolution.

The signal at 0.44 cpd shows high alongshore coherence in currents and hence more reliable phase estimates. Wavelength estimates from current and sea level data range from 790 to 1890 km. The wavelength interval common to current and sea level (1110, 1240 km) has a phase speed interval from 480 to 550 km/day. The wind has a longer wavelength (1270, 2900 km) with higher phase speeds (560, 1280 km/day). There is no single common interval for the wind, sea level, and current estimates.

DISCUSSION

Both linear regression and the spectral analysis supported what seemed obvious from the visual presentation of the observations (Figure 2): that low-frequency fluctuations in the current over the continental shelf are coherent over an alongshore separation of 200 km. In addition, the regression analysis showed that correlation lengths are greater for alongshore than for offshore separations, that the fluctuations are coastally trapped, and that they are correlated with wind and sea level. The spectral analysis showed that the coherent energy occurs mainly at 0.16 cpd, with a lesser peak at 0.3 cpd and an even smaller one at 0.44 cpd.

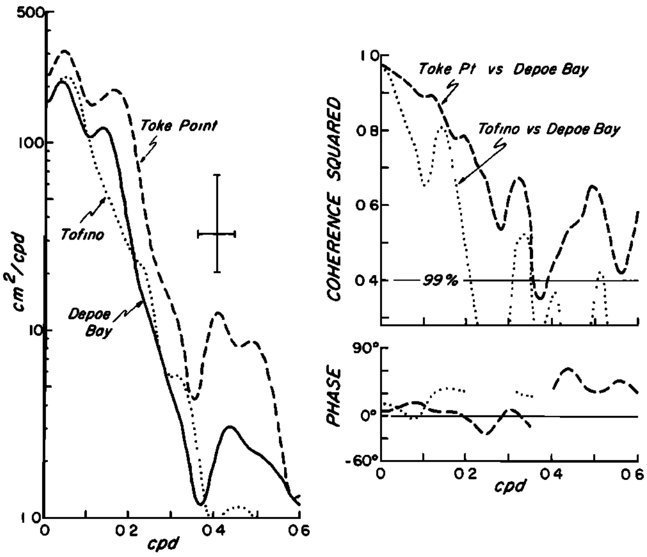

Fig. 8. Autospectra, coherence squared, and phase spectra for sea level observations at Depoe Bay, Oregon; Toke Point, Washington; and Tofino, B. C.

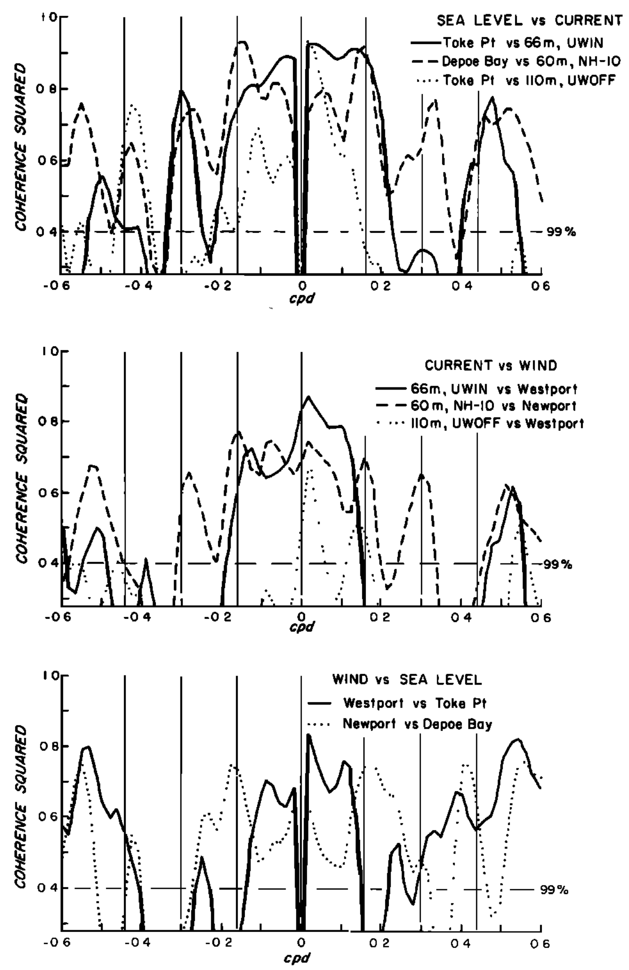

Fig. 9. Coherence squared spectra between sea level, current, and wind, central Oregon and southern Washington.

TABLE 6. Values of Alongshore Coherence Squared (coh²) and Phase ϕ With Its 95% Confidence Limits for Signals at 0.16, 0.3, and 0.44 cpd From Observations of the Deep Inshore Current, Wind, and Sea Level at Locations Separated by a Distance L

		0.16 cpd		0.3 cpd		0.44 cpd	
	L, km	coh²	ϕ, deg	coh²	ϕ, deg	coh²	ϕ, deg
Current (66 m, UWIN; 60 m, NH-10)							
Northward component	200	0.92	23 ± 4	0.51	32 ± 28	0.85	67 ± 9
Alongshore component	200	0.92	21 ± 4	0.58	29 ± 24	0.84	56 ± 9
Major axis component	200	0.89	19 ± 4				
Sea level							
Toke Point, Depoe Bay	210	0.80	7 ± 16	0.59	12 ± 24	0.50	68 ± 28
Tofino, Depoe Bay	490	0.76	36 ± 16	0.27		0.03	
Tofino, Toke Point	280	0.60	36 ± 24	0.24		0.12	
Wind (Westport, Newport)							
Northward component	250	0.77	29 ± 16	0.22		0.66	51 ± 20

Positive phase indicates that the southern observation leads the northern one.

At 0.16 cpd the high mutual coherence between wind, current, and sea level and the similar values of the alongshore coherence of each parameter suggest that the current fluctuations at this frequency may be directly forced by the wind. *Mooers and Smith* [1968] in a study of sea level data obtained in 1933 and 1934 found coupling between atmospheric pressure and sea level at about 0.1 cpd with a predominating period of 6–8 days; they found that the disturbances traveled from north to south between Newport and Brookings, Oregon (at 42°05'N). They concluded that the sea level might simply be reflecting the passage of atmospheric systems. *Gill and Schumann* [1974] suggest that *Mooers and Smith* [1968] observed a forced shelf wave which moves with the wind system. *Smith* [1974] compared wind, sea level, and currents observed at a single location off Oregon in July and August 1972 and found high mutual coherence between wind current and sea level at 0.15 cpd. In a subsequent study of the same observations, *Kundu et al.* [1974] found that this signal has properties consistent with the theoretical results for the resonant response of long barotropic continental shelf waves to an alongshore component of the wind stress propagating northward along the coast as a wave. Our results, indicating similar phase speeds for wind, current, and sea level fluctuations, support their conclusion.

The signal we observed at 0.3 cpd was also found to be present in the 1933–1934 sea level data. *Ma* [1970], using two 100-day data segments, showed it to be stronger in winter than in summer at Coos Bay, Oregon (43°10'N), and Tofino, B.C., and hardly present at San Francisco in either season. He found significant alongshore coherence between Tofino and Coos Bay, separated by 720 km, and interpreted it as a continental shelf wave propagating northward at 700 km/day in winter and 270 km/day in summer. *Mooers and Smith* [1968] also found northward propagation between Brookings, Coos Bay, and Newport with phase differences indicating a phase speed of about 350 km/day. *Cutchin and Smith* [1973] found no evidence of a continental shelf wave at 0.3 cpd in the 1968 observations but apparently observed one at 0.22 and perhaps one at 0.4 cpd. *Smith* [1974] found that his sea level and current spectra suggested the presence of a shelf wave at 0.3 cpd in his 1972 data. *Kundu et al.* [1974] found a signal with a barotropic component at 0.28 cpd in some of the 1973 observations [*Pillsbury et al.*, 1974*b*]. They indicate that the results are consistent with local driving of the currents by the wind stress. Our results indicate that the signal may be generated by the wind off Oregon and that it propagates northward with a phase speed exceeding 630 km/day, much like a continental shelf wave, although it is not strictly barotropic.

The signal at 0.44 cpd may be similar to the one observed at 0.4 cpd by *Cutchin and Smith* [1973], who suggested it might be a second-mode barotropic continental shelf wave. We found its phase speed to be at least 340 km/day and probably about 500 km/day, which is higher than expected (about 150 km/day) for a second-mode continental shelf wave. The signal appears to be somewhat baroclinic: kinetic energy is higher at the shallower current meter (Table 3), and therefore phase speeds based on barotropic shelf wave theory may not be relevant.

Values of correlation and coherence squared between current meters are higher for alongshore separations than for offshore separations, although the alongshore separations are much greater than the offshore separations. Also, the alongshore correlation may depend on the location of both observations; e.g., the alongshore correlation is higher for the inshore pair (UWIN and NH-10) than for the offshore pair (UWOFF and NH-20). Hence care is required in designing experiments to determine the alongshore correlation length scales in currents. Alongshore arrays with moorings on the same isobath do not necessarily yield highest estimates of the alongshore separation: we obtained slightly higher linear correlation between UWIN and NH-20 than between UWIN and NH-10, although UWIN is the shallowest and NH-20 the deepest of the three. Perhaps current meters in even shallower water would yield even higher values of alongshore correlation and coherence. It may be that our observations were at an optimum location. Our results indicate that alongshore coherence is a function of the distance offshore or of the water depth at the mooring sites. Since this function is as yet undetermined, we recommend that any experiment to measure alongshore coherences have an array with two offshore lines of current meter moorings, with at least three moorings in each offshore line, so that the likelihood of severe underestimates of coherence and correlation coefficients will be greatly reduced.

Acknowledgments. We have benefited greatly from the assistance of Joseph Bottero, William E. Gilbert, and Henry Pittock. The current observations were made under National Science Foundation grant ID071-04211 as part of the Coastal Upwelling Ecosystems Analysis (CUEA) program of the U.S. Office of the International Decade of Ocean Exploration (IDOE) and Atomic Energy Commission grant AT (45-1)-2225 (Columbia River Physical Oceanography). Contribution 844 from the Department of Oceanography, University of Washington, Seattle.

REFERENCES

Bakun, A., Coastal upwelling indices, west coast of North America, 1946–71, *Tech. Rep. NMFS SSRF-671,* 103 pp., Nat. Oceanic and Atmos. Admin., Seattle, Wash., 1973.

Cutchin, D. L., and R. L. Smith, Continental shelf waves: Low-frequency variations in sea level and currents over the Oregon continental shelf, *J. Phys. Oceanogr., 3,* 73–82, 1973.

Gill, A. E., and E. H. Schumann, The generation of long shelf waves by the wind, *J. Phys. Oceanogr., 4,* 83–90, 1974.

Gonella, J., A rotary-component method for analyzing meteorological and oceanographic vector time series, *Deep Sea Res., 19,* 833–846, 1972.

Huyer, A., and J. G. Pattullo, A comparison between wind and current observations over the continental shelf off Oregon, summer 1969, *J. Geophys. Res., 77,* 3215–3200, 1972.

Huyer, A., R. D. Pillsbury, and R. L. Smith, Seasonal variation of the alongshore velocity field over the continental shelf off Oregon, *Limnol. Oceanogr., 20,* 90–95, 1975.

Jenkins, G. M., and D. G. Watts, *Spectral Analysis and Its Applications,* 525 pp., Holden-Day, San Francisco, 1968.

Kundu, P. K., J. S. Allen, and R. L. Smith, Modal decomposition of the velocity field near the Oregon coast, submitted to *J. Phys. Oceanogr.,* 1974.

Ma, H. S., Sea level response to low-frequency atmospheric pressure fluctuations along the northwestern American coast, M.S. thesis, 29 pp., Oregon State Univ., Corvallis, 1970.

Mooers, C. N. K., A technique for the cross-spectrum analysis of pairs of complex-valued time series, with emphasis on properties of polarized components and rotational invariants, *Deep Sea Res.,* 20, 1129–1141, 1973.

Mooers, C. N. K., and R. L. Smith, Continental shelf waves off Oregon, *J. Geophys. Res., 73,* 549–557, 1968.

Panofsky, H. A., and G. W. Brier, *Some Applications of Statistics to Meteorology,* 224 pp., Pa. State Univ., University Park, 1963.

Pillsbury, R. D., J. S. Bottero, R. E. Still, and W. E. Gilbert, A compilation of observations from moored current meters, vol. 6, Oregon continental shelf, April to October 1972, *Data Rep. 57 Ref. 74-2,* 230 pp., School of Oceanogr., Oregon State Univ., Corvallis, 1974*a*.

Pillsbury, R. D., J. S. Bottero, R. E. Still, and W. E. Gilbert, A compilation of observations from moored current meters, vol. 7, Oregon continental shelf, July to August 1973, *Data Rep. 58 Ref. 74-7,* 87 pp., School of Oceanogr., Oregon State Univ., Corvallis, 1974*b*.

Smith, R. L., A description of current, wind and sea level variations during coastal upwelling off the Oregon coast, July–August 1972, *J. Geophys. Res., 79,* 435–443, 1974.

(Received January 3, 1975;
accepted March 17, 1975.)